

Critical Heat Flux near the Critical Pressure in Heater Rod Bundle Cooled by R-134a Fluid: Effects of Unheated Rods and Spacer Grid

Se-Young Chun, Chan-Hwan Shin, Sung-Deok Hong and Sang-Ki Moon

Korea Atomic Energy Research Institute, Republic of Korea

E-mail: sychun@kaeri.re.kr

Abstract

In the development of supercritical pressure water cooled reactors, it is important to understand the characteristics of a heat transfer near the thermodynamic critical point. An experimental study on a critical heat flux near the critical pressure has been performed with a 5x5 square array heater rod bundle cooled by R-134a fluid. The critical power has been accurately measured up to a reduced pressure of 0.99 (4.03 MPa). The critical power decreases sharply at a pressure of about 3.8–3.9 MPa as the pressure approaches the critical pressure. The CHF phenomenon near the critical pressure no longer leads to an inordinate increase in the heated wall temperature such as in the case of DNB at normal pressure conditions. In the pressure region close to the critical pressure, there is a threshold pressure at which the CHF phenomenon disappears. When the pressure exceeds this threshold pressure, the wall temperature increases monotonously without a CHF occurrence according to the power level applied to the heater rods. The effect of the unheated rods in the heater rod bundle on the critical power becomes smaller as the pressure approaches the critical pressure. The turbulence effect by the mixing vane of the spacer grid on the critical power is maintained up to a pressure of 3.95 MPa.

Keywords: supercritical-pressure water reactor, near the critical pressure, critical heat flux, R-134a fluid, heater rod bundle, spacer grid, unheated rod

1. Introduction

Research and development efforts for realizing a SuperCritical pressure Water cooled Reactor system (SCWR) are being made at the present time in a number of research institutes (Oka, 2003, Squarer et al., 2003). The SCWRs, which are operated at pressure conditions higher than the thermodynamic critical point of water (374 °C, 22.1 MPa), have advantages over conventional water cooled reactors in terms of thermal efficiency as well as in compactness and simplicity. In conventional water cooled reactors, the critical Heat Flux (CHF) is the most important thermal hydraulic parameter that limits the available core power. The reactor core and nuclear fuel must be designed with an appropriate margin so that the heat flux on the surface of a fuel rod does not exceed the CHF during any condition of a normal operation. On the other hand, since supercritical pressure fluids do not undergo a change of phase, the SCWRs at the rated operating conditions are free from the CHF-related criteria such as the DNBR (DNB heat flux Ratio) and CPR (Critical

Power Ratio) of Light Water Reactors (LWRs). When the SCWRs are operated with a sliding pressure start-up mode, that is, the nuclear heating starts at sub-critical pressures, the CHF should be avoided during the power-increasing phase under sub-critical pressure conditions, just as the power of LWRs is rigidly regulated with the CHF-related criteria. Moreover, in order to ensure the reliability of the safety analyses with computer codes for abnormal pressure decreasing transients including a loss of coolant accident, it is necessary to understand the CHF characteristics near the critical pressure.

A great deal of effort has been expended on experimental and theoretical research on CHF. However, most of the CHF studies have been concentrated on the pressure (up to 17.5 MPa) and flow rate conditions corresponding to the normal operating ranges of LWRs. The large variations in fluid properties near the thermodynamic critical point may lead to different CHF characteristics from that in the normal operating pressures of LWRs. Only a few studies of the CHF near the critical pressure ($P/P_c > 0.90$) have been reported for tubes (Yin et al., 1988, Hong et al., 2004) and the authors recently performed heat transfer experiments with a single heater rod cooled by R-134a (HFC-134a) fluid near the critical pressure in a vertical annular channel (Hong et al., 2004).

Experimental studies in which the CHF has been carefully measured near the critical pressure have not been carried out yet, as far as the authors know. The authors have recently conducted CHF experiments with a 5x5 heater rod bundle cooled by R-134a fluid. It should be noted that the geometry of the rod bundle used in this work differs from the current design of a fuel rod bundle in SCWRs. Therefore, the purpose of this work is to elucidate novel information for a CHF near the critical pressure, based on more accurate experiments. In this paper, the characteristics of the CHF under sub-critical pressure conditions close to the critical pressure are presented, and the effects of the spacer grid with a mixing vane and with the unheated rods on the CHF are discussed.

2. Experimental Description

2.1. Experimental Loop

The experimental work has been performed in the Freon Thermal-Hydraulic Experimental Loop at the Korea Atomic Energy Research Institute (KAERI). This loop uses R-134a ($P_c = 4.059$ MPa, $T_c = 101$ °C) as a working fluid and can be operated up to 4.50 MPa (water equivalent pressure, which is determined from the same reduced pressure, is 24.49 MPa.) and 160 °C. Figure 1 shows a simplified flow diagram of the Freon loop. It basically consists of a circulating pump, a preheater, a pressurizer, a vertical test section, a vapor/liquid separator, a condenser and a cooler. The R-134a fluid is circulated in the main loop by a canned motor centrifugal pump. The flow rate through the test section inlet is controlled by adjustments of the circulating pump motor speed, the flow control valve and the bypass valve. The flow rate at the test section is measured by a Coriolis-type mass flow meter. The fluid temperature at the test section inlet is finely adjusted by the preheater. The two-phase flow mixture from the test section is separated into vapor and liquid in the separator. The separated vapor is condensed while flowing through a condenser attached to the separator.

An accumulator is used as the pressurizer, which controls the loop pressure by using Nitrogen gas. The power applied to the test section is supplied from a 60 volts x 12000 amperes, dc (direct-current) power source.

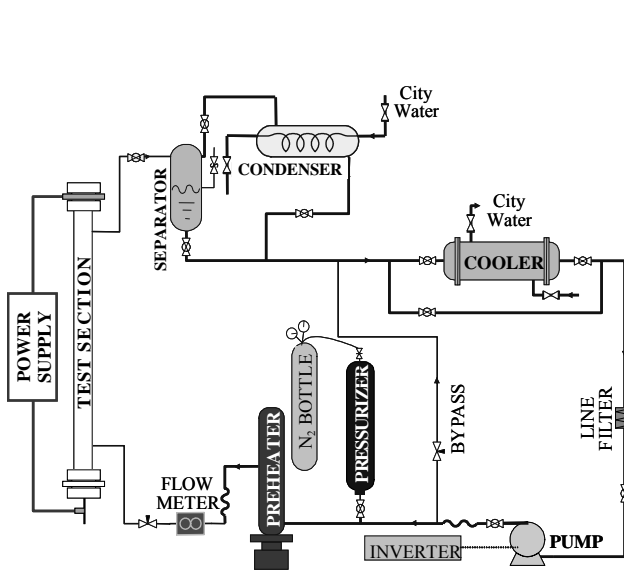


Fig. 1 Schematic diagram of the experimental loop

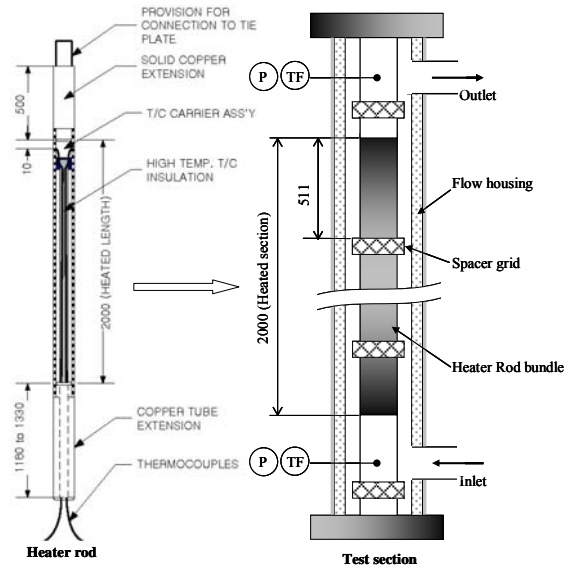


Fig. 2 Configuration of the test section

2.2. Test Section

Figure 2 shows the configuration of the test section and a sketch of the heater rod. The cross-sectional view of the heater rod bundle and the spacer grids used in the present work is shown in Fig. 3. The heater rod bundle in a 5x5 square array is installed in a ceramic flow housing inside the pressure vessel. The heater rods are made of Inconel 601 tube with an outer diameter of 9.5 mm and a heated length of 2000 mm at room temperature, and are directly heated by a large direct-current passing through the heater wall. The spacing between the heater rods is maintained at a rod pitch of 12.85 mm by the spacer grids. Three kinds of heater rod bundles have been used in the present experiments; (TS-1): the heater rod bundle with the plain spacer grids, (TS-2): with the mixing vane spacer grids, (TS-3): with the plain spacer grids and the four unheated rods. For measuring the heater rod wall temperatures and detecting the CHF occurrence, K-type thermocouples with a sheath outer diameter of 0.5 mm are attached to the inside wall surface of the heater rod. All the thermocouples for the wall temperature are located at 10 mm below the top end of the heated section, since the CHF in a vertical upward flow with an axially uniform heat flux always occurs at the top end of the heated section. The radial power distribution of the rod bundle is non-uniform. The power of the middle rods including a central rod is approximately 20 % higher than that of the peripheral rods including the four corner rods as shown in Fig. 3. Each of the middle rods contains four thermocouples, while two thermocouples are mounted on each of the other rods. In Fig. 3, the numbers inside the heater rod circles and the small numbers outside the circles denote the power factor and the thermocouple locations, respectively. The power factor is defined as the ratio of the

local heater rod power to the average rod power of the heater rod bundle.

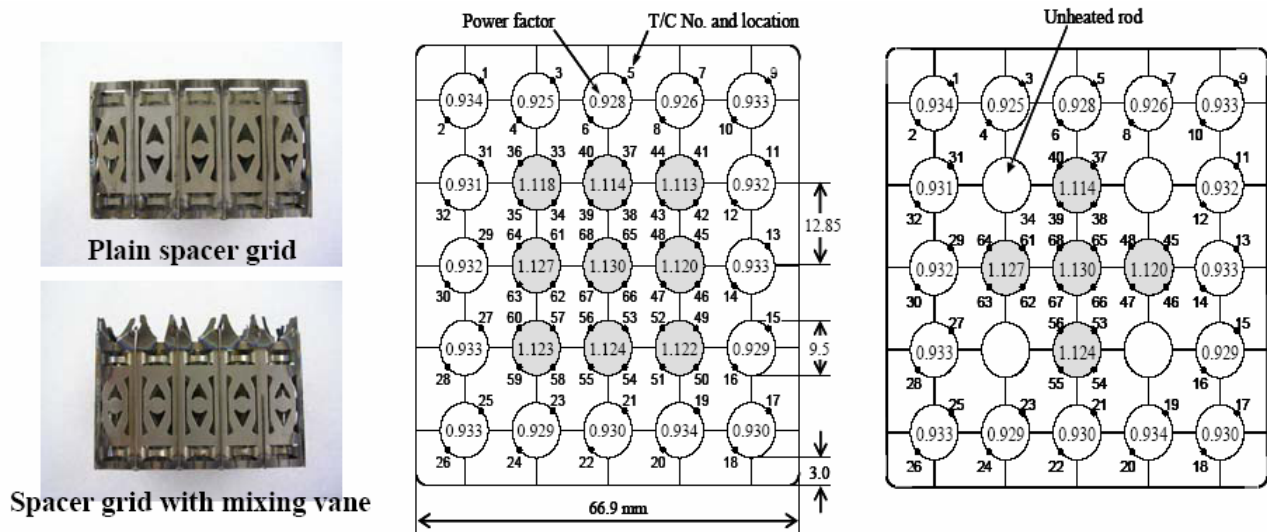


Fig. 3 Spacer grids and a cross-sectional view of a 5x5 heater rod bundle

2.3. Experimental Procedure and Conditions

First, the flow rate, inlet subcooling and system pressure (at the test section outlet) are set to the desired levels, and then power is applied to the heater rod bundle of the test section and increased gradually in small steps. An appropriate time interval between the power steps is applied so that the experimental parameters such as the flow rate, inlet temperature, and system pressure can be stabilized at steady state conditions. This process is continued until a sharp increase in the wall temperatures of the heater rods is observed. In the sub-critical pressure region close to the critical pressure, the pressure was adjusted very carefully because a slight change of the pressures could lead to a relatively large change of the CHF value. In the present experiments, the CHF is defined as the heat flux at the time when one of the wall temperatures of the heater rods shows a sharp increase. The CHF detection and protection system continuously scans the temperature signals from all the thermocouples. When the wall temperature reaches the pre-determined set point, the dc power to the heater rod bundle is automatically decreased or tripped by the power run down/trip system.

For performing the experiments and analyzing the experimental data, the thermodynamic properties of R-134a from the NIST (National Institute of Standards and Technology) REFPROP version 6.01 (MaLinden et al., 2003) have been used. The present work has focused on the following conditions:

- system pressure 3.00 to 4.03 MPa (reduced pressure: $P/P_c=0.74-0.99$)
- mass flux 50 to 2000 $\text{kg/m}^2\text{s}$
- inlet subcooling 40, 55, 70 and 84 kJ/kg

The inlet subcooling is determined from the fluid temperature and the pressure at the inlet plenum of the test section. In this work, the system pressure is the pressure at the outlet plenum of the test

section.

The uncertainties of the measuring system were estimated from a calibration of the sensors and the accuracy of the equipment, according to a propagation error analysis based on the Taylor's series method (ANSI/ASME PTC 19.1, 1985). The evaluated maximum uncertainties of the pressures, flow rates, and temperatures are less than $\pm 0.25\%$, $\pm 0.6\%$ and $\pm 0.7\text{ }^\circ\text{C}$ of the readings in the range of interest, respectively. The uncertainty of the power calculated from the voltage and current applied to the heater rod bundle is always less than $\pm 1.8\%$ of the readings. The heat loss in the test section is taken into account in the calculation of the power. Before starting a set of experiments, pretests (*i.e.*, heat balance tests) were carried out to estimate the heat loss from the test section. The heat losses estimated by the pretests for each pressure condition are less than 1.0% of the power input.

3. Experimental Results and Discussions

3.1. Characteristics of CHF for the Rod Bundle with the Plain Spacer Grids

In this paper, the critical power Q_{CHF} , which is defined as the total power applied to the heater rod bundle at CHF occurrence, is dealt with instead of a local CHF to avoid the complexity attributed to a non-uniformly radial power distribution. Figure 4 shows the effect of the mass flux on the critical power with the pressure as a parameter, together with the complete evaporation lines, which are calculated from heat balance consideration for a thermodynamic quality equal to 100% . The critical power increases rapidly at low mass fluxes and slowly at high mass fluxes with increasing mass flux, and it increases monotonously up to a high mass flux (about $2000\text{ kg/m}^2\text{s}$) for the mass fluxes exceeding approximately $500\text{ kg/m}^2\text{s}$. This trend is the same as that of the CHF data from a previous experimental work (Moon et al., 2005) at normal pressures. The slope of the increasing critical power curve $(\Delta Q_{CHF})/(\Delta G)$ becomes gentle as the pressure increases. As shown in Fig. 4, the critical power is little affected by the pressure at a mass flux of $50\text{ kg/m}^2\text{s}$. Under low flow rate conditions, it is presumed that the CHF mechanism is mainly subject to the dryout of a liquid film in annular flow. The entrainment of a liquid droplet in annular flow does not occur actively at a very low flow rate. In this case, the CHF may be primarily governed by the evaporation of the liquid film. The generation of an entrainment is activated at the higher mass flux conditions. Consequently, the critical power at very low mass fluxes of 50 and $150\text{ kg/m}^2\text{s}$ is close to the complete evaporation lines, and as the mass flux increases, the curves of the critical power move away from the complete evaporation lines.

For the influence of the system pressure, the CHF for a water flow in a tube and annulus decreases monotonously with increasing pressure in the range of about 4 to 17 MPa (Yin et al., 1988, Chun et al., 2000). Figure 5 shows the critical power as a function of the pressure with the inlet subcooling as a parameter. The critical power decreases monotonously up to a pressure of about $3.6\text{--}3.8\text{ MPa}$ with increasing pressure, and then it falls sharply at about $3.8\text{--}3.9\text{ MPa}$ as if the values of the critical power converge to zero at the critical pressure (4.059 MPa). This sharp

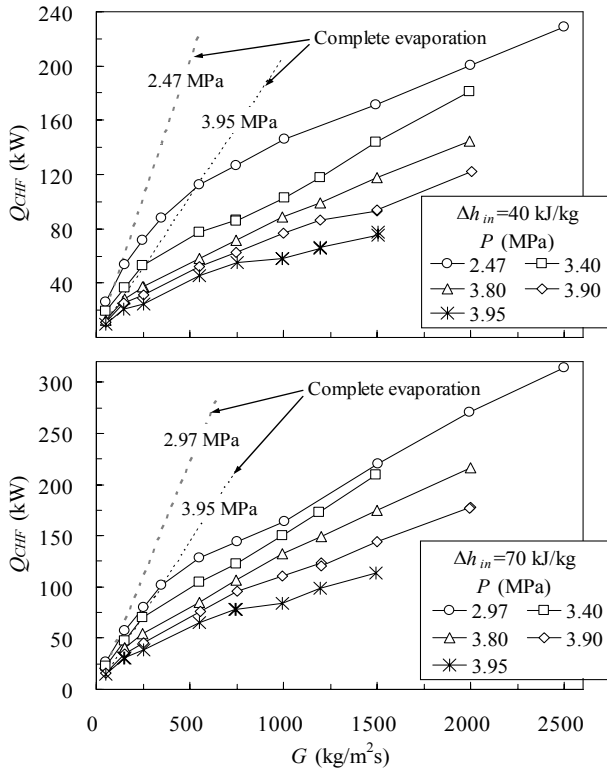


Fig. 4 Critical power as a function of the mass Flux (TS-1)

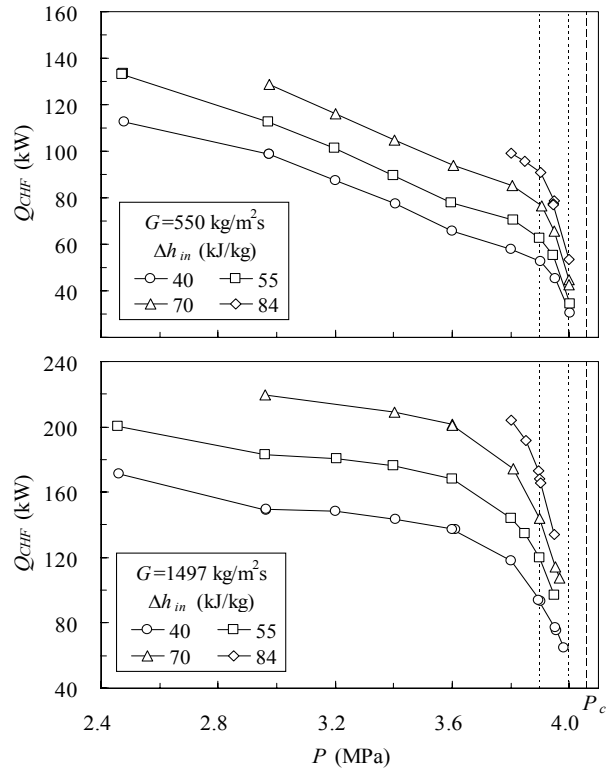


Fig. 5 Critical power as a function of the pressure at a fixed mass flux (TS-1)

decreasing trend of the critical power occurs more strongly when the inlet subcooling is increased. The trend mentioned above was also observed in the water experiments in a tube by Yin, et al., 1988 and in the R-134a experiments in an annulus by Hong et al., 2004.

CHF is frequently related to the critical quality x_{CHF} , which is the thermodynamic quality at the location of a CHF occurrence. Characteristics of a heat transfer near the critical pressure are closely related to the thermodynamic properties of a fluid. Therefore, the critical quality, together with the saturated densities ρ , the latent heat of vaporization h_{lv} and the specific heat of a saturated liquid C_{pl} for R-134a, with increasing pressure is shown in Fig. 6. The scale of the y-axis for the latent heat, densities and specific heat is chosen arbitrarily. The values of a critical quality decrease slowly up to the pressure of 3.8 MPa as the pressure increases. When the pressure exceeds 3.8 MPa, the critical quality starts to decrease suddenly and the thermodynamic properties start to vary greatly. The critical qualities show fairly large negative values at the pressures very close to the critical pressure, because the CHF occurs at a considerably lower power and the latent heat reaches zero at the critical pressure. It is especially notable that a sharp decrease of the critical power and the latent heat commences at almost the same pressure. It can be speculated that the sharp decrease of the critical power might be caused by the decrease of the latent heat. In the present experiments, for the pressures above 3.6 MPa, a CHF occurred invariably at negative values of the quality, except for that for the mass fluxes of less than $550 \text{ kg/m}^2\text{s}$. On the other hand, the critical quality for the mass fluxes of 50 and $150 \text{ kg/m}^2\text{s}$ has positive values up to a pressure of 4.0 MPa.

The general consensus is that in a flow boiling, the physical mechanism of a CHF in a normal pressure region can be classified into a DNB and a liquid film dryout. The DNB occurs when the bulk liquid is subcooled or at a low quality and is characterized by a rapid rise in the heated wall temperature. Liquid film dryout occurs in an annular flow or an annular-mist flow under high quality conditions and the heated wall temperature rises comparatively slowly with its oscillations. As mentioned above, much of the critical quality for the pressures above 3.6 MPa has a negative value, namely a CHF occurs under subcooled conditions. Figure 7 shows the difference in the wall temperature variations depending on the pressure at CHF conditions. According to the conventional view of the CHF characteristics mentioned above, the temperature variations at T/C64 and 47 for the mass flux of 1497 kg/m²s, at T/C67 and T/C66 for the mass fluxes of 996 and 550 kg/m²s, respectively, show typical DNB characteristics. For the pressures of 3.95–4.00 MPa, the behavior of the temperatures at T/C52 for the mass fluxes of 1497 and 996 kg/m²s, and at T/C30 for the mass flux of 550 kg/m²s indicate the features of a liquid film dryout rather than a DNB, although the boiling system is under highly subcooled conditions. This implies that the CHF phenomenon near the critical pressure no longer leads to an inordinate increase in the heated wall temperature such as in the case of a DNB at normal pressure conditions. Furthermore, when the pressure approaches 3.98–4.03 MPa, very close to the critical pressure, the CHF phenomenon disappears. In Fig. 7, the wall temperatures designated by A, B and C increase monotonously without a CHF occurrence according to the applied power level while the applied power is increased beyond the expected critical power.

Figure 8 shows the critical power as a function of the pressure with the mass flux as a parameter for a fixed inlet subcooling. The behavior of the critical power with the pressure for the mass fluxes of not less than 550 kg/m²s shows the same decreasing trend as that in Fig. 5. As the mass flux decreases, the slope of the decreasing critical power becomes gentle. For the low mass fluxes of 50 to 249 kg/m²s, a sharp decrease of the critical power near the critical pressure is not observed. It is seen from the comparison between Fig. 5 and 8 that the mass flux rather than the inlet subcooling has a greater effect on the behavior of the critical power near the critical pressure. The authors have found the existence of a pressure region in which the CHF phenomenon does not occur. In Fig. 8, the dotted lines indicate a threshold pressure at which the CHF phenomenon disappears. As the pressure approaches the critical pressure, the critical power decreases and the increase of the wall temperature at the CHF occurrence becomes smaller (see Fig. 7). When the pressure passes through the Threshold Pressure Line (TPL), the CHF phenomenon cannot be identified. The solid data points in Fig. 8 designate the power which has been applied to the heater rod bundle beyond the expected critical power without a CHF occurrence. The data points A, B and C correspond to the wall temperature variations of A, B and C in Fig. 7, respectively. The threshold pressure moves toward the lower pressure region gradually as the mass flux is increased. As can be seen from Fig. 7, the threshold pressure is little affected by the inlet subcooling, although it seems that an inlet subcooling has an effect on the threshold pressure for the high mass flux of 1497 kg/m²s.

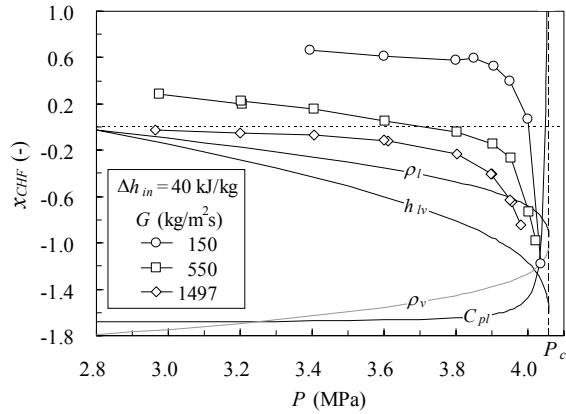


Fig. 6 Critical quality and thermodynamic properties with the pressure (TS-1)

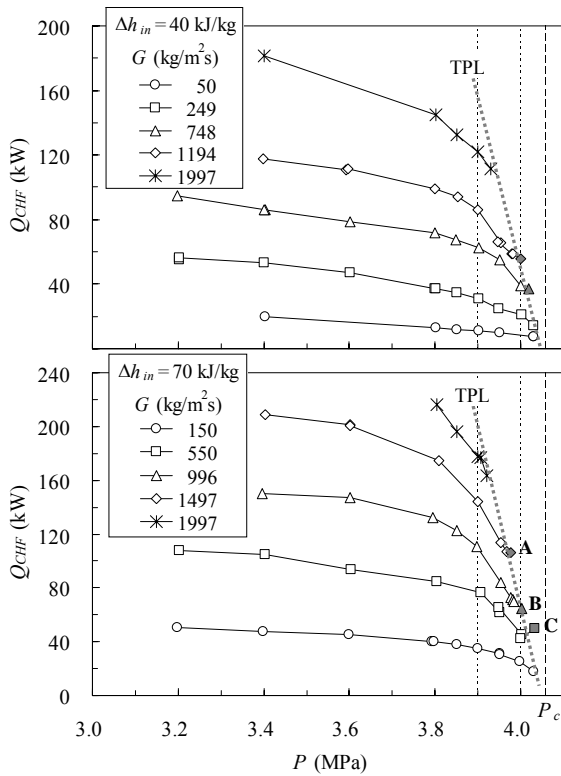


Fig. 8 Critical power as a function of the pressure at a fixed inlet subcooling (TS-1)

3.2. Effects of Unheated Rods and Spacer Grid on CHF

In order to investigate the effects of the spacer grid and the unheated rods on the CHF, the critical power data in the heater rod bundles with mixing vane spacer grids (TS-2) and with the four unheated rods and the plain spacer grids (TS-3) have been compared with those for the heater rod bundle with the plain spacer grids (TS-1). Figure 9 shows the comparison of the critical power data in TS-1 and TS-2. The critical power of the heater rod bundle with the mixing vane spacer grids shows larger values when compared to that for the spacer grids without mixing vanes (the plain

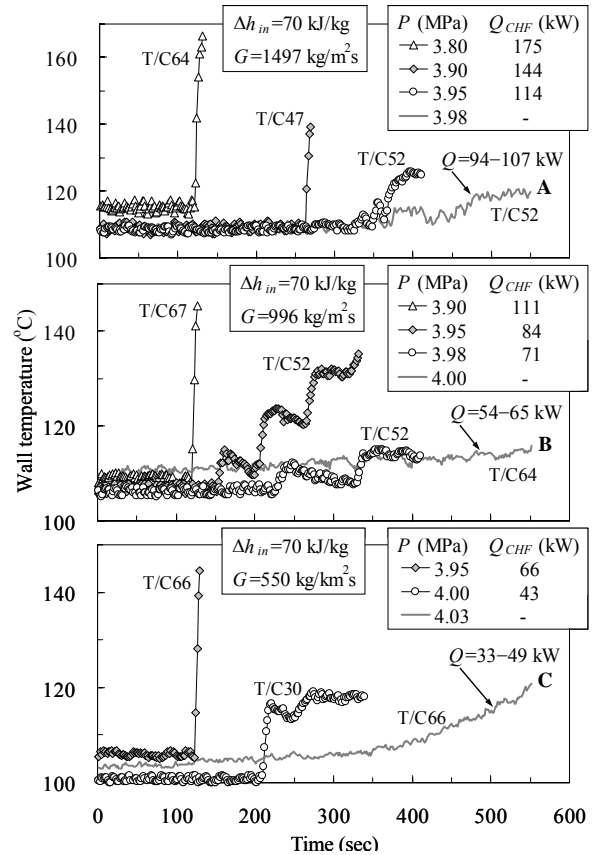


Fig. 7 Difference in the wall temperature variations depending on the pressure (TS-1)

spacer grids). This trend is maintained up to a pressure of 3.95 MPa ($P/P_c = 0.97$) very close to the critical pressure. Figure 10 shows the comparison of the critical power data in TS-1 and TS-3. For the high mass fluxes of 998 and 1497 kg/m²s, the effect of the unheated rods in the heater rod bundle on the critical power becomes smaller as the pressure approaches the critical pressure, and when the pressure exceeds 3.9 MPa, the unheated rods have little effect on the critical power. In the case of the low mass fluxes of 150 and 548 kg/m²s, it is seen from Fig. 10 that the critical power is not influenced by the unheated rods.

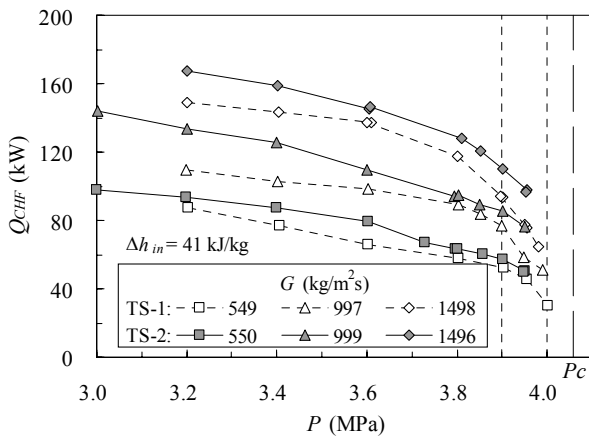


Fig. 9 Critical power as a function of the pressure: TS-1 versus TS-2

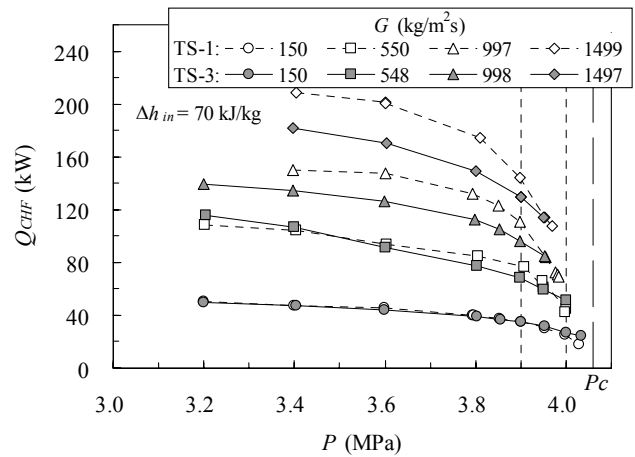


Fig. 10 Critical power as a function of the pressure: TS-1 versus TS-3

4. Conclusions

In order to understand the CHF characteristics near the critical pressure, experiments were performed with a 5x5 heater rod bundle cooled by R-134a fluid. The critical power has been measured more carefully up to the pressures very close to the critical pressure. The following conclusions can be drawn from this study:

- (1) For the mass fluxes of not less than 550 kg/m²s, the critical power decreases slowly up to a pressure of about 3.8 MPa with increasing pressure, and then it falls sharply at about 3.9 MPa. This sharp decreasing trend of the critical power is more prominent when the inlet subcooling and/or the mass flux are increased. For the low mass fluxes of 50 to 249 kg/m²s, a sharp decrease of the critical power is not observed near the critical pressure.
- (2) When the pressure becomes very close to the critical pressure, the critical quality also drops sharply to a large negative value, that is, the flow at the CHF occurrence is under highly subcooled conditions. However, the CHF phenomenon no longer leads to an inordinate increase in the heated wall temperature such as in the case of a DNB at normal pressure conditions.
- (3) The existence of a threshold pressure at which the CHF phenomenon disappears has been observed in the sub-critical pressure region near the critical pressure. When the pressure exceeds the threshold pressure, a CHF does not occur and the wall temperature increases monotonously without the CHF occurrence according to the power level applied to the heater rod bundle.

(4) The critical power of the heater rod bundle with the mixing vane spacer grids shows larger values when compared to that for the plain spacer grids. This trend is maintained up to a pressure of 3.95 MPa. The effect of the unheated rods on the critical power becomes smaller as the pressure approaches the critical pressure, and when the pressure exceeds 3.9 MPa, the unheated rods have little effect on the critical power.

Nomenclature

C_{pl}	specific heat of saturated liquid (kJ/kgK)	Q_{CHF}	critical power defined as the power applied to the heater rod bundle at CHF occurrence (kW)
G	mass flux (kg/m ² s)	T_c	critical temperature (°C)
h_{lv}	latent heat of vaporization (kJ/kg)	x_{CHF}	critical quality, that is, thermodynamic quality at CHF occurrence location (-)
Δh_{in}	inlet subcooling (kJ/kg)	ρ_l	density of saturated liquid (kg/m ³)
P	system pressure (MPa)	ρ_v	density of saturated vapor (kg/m ³)
P_c	critical pressure (MPa)		
Q	power applied to the heater rod bundle (kW)		

Acknowledgements

This study has been carried out under the Nuclear R & D Program supported by the Ministry of Science and Technology (MOST) of Korea.

References

- ANSI/ASME PTC 19.1, 1985, "ASME Performance Test Codes, Supplement on instruments and apparatus, part 1, measurement uncertainty," ASME, New York.
- Chun, S. Y., Chung, H. J., Hong, S. D. et al., 2000, "Critical heat flux in uniformly heated vertical annulus under a wide range of pressures-0.57 to 15.0 MPa," *J. Korean Nuclear Society*, **32**[2], 128.
- Hong, S. D., Chun, S. Y., Kim, S. Y. et al., 2004, "Heat transfer characteristics of an internally-heated annulus cooled with R-134a near the critical pressure," *J. Korean Nuclear Society*, **36**[5], 403.
- MaLinden, M. O., Klein, S. A., Lemmon, E. W. et al., 2003, "REFPROP, Thermodynamic and Transport Properties of Refrigerants and Refrigerant Mixtures," NIST Standard Reference Database 23-Version 6.01, National Institute of Standards and Technology.
- Moon, S. K., Chun, S. Y., Cho, S. et al., 2005, "An experimental study on the critical heat flux for low flow of water in a non-uniformly heated vertical rod bundle over a wide range of pressure conditions," *Nucl. Eng. Des.*, **235**, 2295.
- Oka, Y., 2003, "Research and development of the supercritical-pressure light water cooled reactors," *Proc. 10th Int. Topical Meeting on Nuclear Reactor Thermal Hydraulics (NURETH-10)*, Seoul, Korea, Paper KL-02.
- Squarer, D., Schulenberg, T., Struwe, D. et al., 2003, "High performance light water reactor," *Nucl. Eng. Des.*, **221**, 167.

Yin, S., Lui, T. J., Huang, Y. D. et al., 1988, "Measurements of critical heat flux in forced flow at pressures up to the vicinity of the critical point of water, *Proc. 1988 National Heat Transfer Conf.*, U.S.A., Houston, U.S.A, July 24-27, **1**, 501.